Molecular Biology of the Cell
Vol. 15, 4609–4621, October 2004

Enhanced Membrane Fusion in Sterol-enriched Vacuoles Bypasses the Vrp1p Requirement[D]

Kelly Tedrick,* Tim Trischuk,† Richard Lehner,*† and Gary Eitzen*‡

*Department of Cell Biology and †CIHR Group on the Molecular and Cell Biology of Lipids, University of Alberta, Edmonton, Alberta, T6G 2H7 Canada

Submitted March 9, 2004; Accepted July 1, 2004
Monitoring Editor: David Drubin

Organization of lipids into membrane microdomains is a vital mechanism of protein processing. Here we show that overexpression of *ERG6*, a gene involved in ergosterol synthesis, elevates sterol levels 1.5-fold on the vacuole membrane and enhances their homotypic fusion. The mechanism of sterol-enhanced fusion is not via more efficient sorting, but instead promotes increased kinetics of fusion subreactions. We initially isolated *ERG6* as a suppressor of a *vrp1*Δ growth defect selective for vacuole function. *VRP1* encodes verprolin, an actin-binding protein that colocalizes to vacuoles. The *vrp1*Δ mutant has fragmented vacuoles in vivo and isolated vacuoles do not fuse in vitro, indicative of a Vrp1p requirement for membrane fusion. *ERG6* overexpression rescues *vrp1*Δ vacuole fusion in a cytosol-dependent manner. Cytosol prepared from the *vrp1*Δ strain remains active; therefore, cytosol is not resupplying Vrp1p. Las17p (Vrp1p functional partner) antibodies, which inhibit wild-type vacuole fusion, do not inhibit the fusion of vacuoles from the *vrp1*Δ*-ERG6* overexpression strain. Vacuole-associated actin turnover is decreased in the *vrp1*Δ strain, but recovered by *ERG6* overexpression linking sterol enrichment to actin remodeling. Therefore, the Vrp1p/Las17p requirement for membrane fusion is bypassed by increased sterols, which promotes actin remodeling as part the membrane fusion mechanism.

INTRODUCTION

A hallmark of the eukaryotic cell is the compartmentalization of metabolic processes. To maintain compartment identity the cell utilizes transport vesicles that deliver cargo to correct destinations. Overlapping regulatory mechanisms control the fidelity of vesicle docking and membrane fusion (Jahn and Sudhof, 1999). The specificity of vesicle docking is controlled by a diverse set of proteins with both Rab and Rho GTPases acting as master regulators (Segev, 2001; Symons and Rusk, 2003). SNARE (soluble N-ethylmaleimide-sensitive factor attachment protein receptor) proteins are key players in the membrane fusion process; however, it is still a matter of debate whether SNAREs act at the final step of bilayer mixing (Mayer, 2002; Jahn *et al.,* 2003).

Vacuole membrane fusion can serve as a paradigm for vesicular trafficking because much of the protein enzymology and lipid requirements have been well documented (Wickner, 2002). Recent reports have detailed the importance of local membrane microdomains that form in response to signals generated by vesicle docking (Wang *et al.,* 2002). These authors found domains at the vertices of docked membranes enrich in fusogenic proteins, and provide the site at which membrane fusion is catalyzed. The assembly of these domains was subsequently shown to be an active process requiring lipid molecules and actin remodeling (Wang *et al.,* 2003).

We are interested in further defining the role of actin in membrane fusion and identifying components of the signaling pathway that controls actin remodeling. An actin-remodeling requirement has been implicated in several membrane fusion systems (Stamnes, 2002; Eitzen, 2003), but the precise role of actin during fusion is still a matter of debate. Current data clearly support roles for F-actin polymerization (Jahraus *et al.,* 2001; Kjeken *et al.,* 2004), depolymerization (Vitale *et al.,* 1991; Muallem *et al.,* 1995), or both (Bernstein *et al.,* 1998; Eitzen *et al.,* 2002). Signaling pathways exist on membranes of isolated organelles that control actin assembly (Defacque *et al.,* 2000; Eitzen *et al.,* 2002). Recently several reports have also defined a role for lipids in the regulation of actin cytoskeleton remodeling in conjunction with vesicular trafficking (Zanolari *et al.,* 2000; Friant *et al.,* 2000, 2001; Anes *et al.,* 2003).

The significance of local membrane structure in vesicular traffic is also manifested in the importance of lipid raft formation (Ikonen, 2001). Lipid rafts are sterol-sphingolipid–enriched membrane subdomains that are resistant to detergent solubilization. These domains selectively recruit proteins providing a basis for the formation of distinct mechanistic complexes within membranes. Though organization of the membrane into rafts has received much attention lately, nonraft membrane subdomains enriched in specific lipids have also been shown important (Anderson and Jacobson, 2002). Therefore, a study of the signaling pathway for actin remodeling during membrane fusion, will ultimately involve a role in lipid microdomain formation.

In this report we provide links between ergosterol (the yeast equivalent of cholesterol), the cytoskeleton, and membrane fusion. Disruption of ergosterol synthesis causes defects in endocytosis and vacuole biogenesis (Munn *et al.,*

Article published online ahead of print. Mol. Biol. Cell 10.1091/mbc.E04–03–0194. Article and publication date are available at www.molbiolcell.org/cgi/doi/10.1091/mbc.E04–03–0194.

[D] The online version of this article contains supplemental material accessible through http://www.molbiolcell.org.

‡ Corresponding author. E-mail address: gary.eitzen@ualberta.ca. Website: www.ualberta.ca/CELLBIOLOGY/eitzen.html.

Table 1. Strains used in this study

DDY2246[d]	*LAS17::LEU2, ade2, his3, leu2, ura3, lys2*
DDY2266[d]	*las17–16::LEU2, ade2, his3, leu2, ura3, lys2*
GEY0394[b]	BY4742, *pep4::kanMX, ACT1::HIS3*
GEY0394-101[b]	BY4742, *pep4::kanMX, act1-101::HIS3*
GEY0394-157[b]	BY4742, *pep4::kanMX, act1-157::HIS3*
K91[b]	*pho8::URA3, pho4::LEU2*
KTY1[a]	*pep4::kanMX, prb1::LEU2*
KTY2[a]	*pho8::kanMX*
KTY3[a]	*pep4::kanMX, prb1::LEU2, His3MX6-*P_{GAL1}-3HA::*ERG6*
KTY4[a]	*pho8::kanMX, His3MX6-*P_{GAL1}-3HA::*ERG6*
KTY5[a]	*vrp1::kanMX, pep4::URA3, prb1::LEU2*
KTY6[a]	*vrp1::kanMX, pho8::URA3*
KTY7[a]	*vrp1::kanMX, pep4::URA3, prb1::LEU2, His3MX6-*P_{GAL1}-3HA::*ERG6*
KTY8[a]	*vrp1::kanMX, pho8::URA3, His3MX6-*P_{GAL1}-3HA::*ERG6*
KTY10[a]	*vrp1::kanMX*
KTY11[a]	*vps33::kanMX*
KTY12[a]	*ypt7::kanMX*
KTY13[a]	*vps5::kanMX*
KTY14[a]	*vam3::kanMX*
KTY15[a]	*erg6::kanMX*
KTY10-0[a]	*vrp1::kanMX*, YEp13::Ch. XII 801550–806600 (p*VRP1*g)
KTY10-16[a]	*vrp1::kanMX*, YEp13::Ch. XIII 251700–257000 (p*ERG6*g)
KTY10-40[a]	*vrp1::kanMX*, YEp13::Ch. XV 675750–680800 (p*LAS17*g)
RH1745[c]	*ARC35, leu2, ura3, his4, bar1*
RH2616[c]	*arc35-1, leu2, ura3, his4, bar1*

Sources: [a] This study using base strain BY4742 (*his3, leu2, ura3, lys2*) and *kanMX* disruptions obtained from Research Genetics; [b] obtained from W. Wickner (Haas, 1995; Eitzen *et al.*, 2002); [c] obtained from H. Riezman (Schaerer-Brodbeck and Riezman, 2000); [d] obtained from D. Drubin (Duncan *et al.*, 2001). All strains are mating type alpha.

1999; Kato and Wickner, 2001; Heese-Peck *et al.*, 2002). We now show that vacuolar sterol enrichment via upregulation of *ERG6*, a late gene in the ergosterol synthesis pathway, suppresses growth defects caused by *VRP1* gene deletion or *LAS17* gene mutation, both components of the actin remodeling machinery (Evangelista *et al.*, 2000). Morphological defects of vacuole fragmentation in the *vrp1*Δ strain were rescued via *ERG6* overexpression, and in vitro studies showed sterol enrichment and greatly enhanced vacuole membrane fusion.

MATERIALS AND METHODS

Yeast Strains, Growth, and Genetic Modification

Yeast strains are listed in Table 1. Yeast were grown in 1% yeast extract, 2% peptone (YP), supplemented with dextrose and/or galactose as indicated. For isolation of suppressor genes, KTY10 (*vrp1*Δ) was transformed by electroporation (Ausubel *et al.*, 1989) with a genomic library in YEp13 (ATCC 37323). Approximately 10^4 colonies were grown on CSM-leucine (BIO 101, Carlsbad, CA) agar plates and replica plated onto YPD (YP supplemented with 2% dextrose) supplemented with 6 mM caffeine. DNA was isolated from colonies growing after 4 d, plasmids were purified by *Escherichia coli* transformation and inserts were partially sequenced. Clones were identified by database search and the significant hits are listed in Figure 1B. The *ERG6* open reading frame with ~200 base pairs of upstream and downstream sequence was subcloned into pRS425/426 (p*ERG6*-2μ) and pRS315/316 (p*ERG6*-cen) as a *Bam*HI fragment using primers 5′ERG6 and 3′ERG6 (Table 2). To examine suppression of growth defects, strains were transformed by electroporation with empty plasmids or plasmids containing the *ERG6* gene and plated as a 10-fold dilution series on YPD media containing either 6 mM caffeine or 1.8 M sorbitol where indicated. Cultures shown on YPD-only plates were initially diluted an additional 10-fold to improve the comparison. Gene deletions were performed by homologous recombination of PCR products using primers with ~40 nucleotides of homology to the 5′ and 3′ ends of the gene of interest (Table 2) and 20 nucleotides of homology to the pRS 40× vector series as the template (Brachmann *et al.*, 1998). The *GAL1* promoter and three HA epitopes were inserted at the 5′ end of the *ERG6* open reading frame by homologous recombination using a PCR product generated with primers F4-ERG6 and R3-ERG6 (Table 2) and template plasmid pFA6a-His3MX6-PGAL1-3HA (Longtine *et al.*, 1998). Growth curves were generated for strains by diluting overnight cultures to 1 OD_{600} and adding 0.1 ml to 50 ml of fresh media. Vacuole morphology was examined by adding 1 μl of 8 mM FM4-64 (Molecular Probes, Eugene, OR) to 0.2 ml of culture at 1 OD_{600}. Cells were reisolated after 15 min, supplemented with 1 ml fresh medium, and incubated for 3 h before examination by fluorescence microscopy using an Axioskop2 microscope (Zeiss, Thornwood, NY) equipped with a Spot1.1 digital camera (Diagnostic Instruments, Sterling Heights, MI).

Protein Processing and Analysis

Whole cell lysates to analyze protein levels were prepared as follows. Cell cultures were grown to 1 OD_{600}, 0.25 ml was harvested, washed with water, and incubated 10 min in 575 μl of 240 mM NaOH, 140 mM β-mercaptoethanol, 1.5 mM PMSF. Proteins were precipitated by adding 575 μl of 50% TCA, incubated 10 min at 4°C, and centrifuged at 20,000 × *g* for 15 min at 4°C followed by an 80% acetone wash. Samples were resuspended in 60 μl of sample buffer (62.5 mM Tris-Cl, pH 6.8, 10% [vol/vol] glycerol, 2% [wt/vol] SDS, 140 mM β-mercaptoethanol) and analyzed by SDS-PAGE and immunoblotting. Sec17p release assays were performed as previously described (Mayer *et al.*, 1996) except that 5 μg/ml recombinant Sec18p was also added. Vacuole-bound actin was examined over the course of standard fusion reactions without the addition of cytosol to limit rebinding. At specified times, vacuoles (with associated actin) were diluted fivefold in FRB (fusion reaction buffer; see below) and precipitated by centrifugation at 20,000 × *g* for 5 min at 4°C. Equal fractions were analyzed by SDS-PAGE and immunoblot. Immunoblots band intensities were quantified by densitometry; corrections for small variations in gel loading were made by first calculating the ratio of band intensities of the variable (actin or Sec17p) to the band intensities of the vacuole membrane marker, alkaline phosphatase, which remains unchanged during experiments. Membrane-associated and integral membrane proportion of protein was determined by incubation of 100 μg of total vacuolar protein in 0.2 ml of 50 mM Tris-Cl, pH 8.5, or 100 mM Na_2CO_3, pH 11.5, buffers, respectively, for 15 min at 4°C followed by centrifugation at 100,000 × *g* for 30 min at 4°C. The amount of precipitated protein was determined by Bradford assay and expressed as a percentage of total in Table 3. Extracellular CpY was analyzed by secretion filter binding assay as described (Roberts *et al.*, 1991). Briefly, 3 μl of a 10-fold dilution series was plated onto YPD or 1% galactose/0.2% dextrose (YPG), overlaid with nitrocellulose filters, incubated for 48 h at 28°C, and then immunoblotted for CpY. Immunoblots were processed using an Odyssey digital imaging system (Li-Cor, Lincoln, NE) with resolution set to 84 μm and highest quality. Secondary antibody used was IRDye800-conjugated goat anti-rabbit/-mouse antibodies (Rockland Immunochemicals, Gilbertsville, PA).

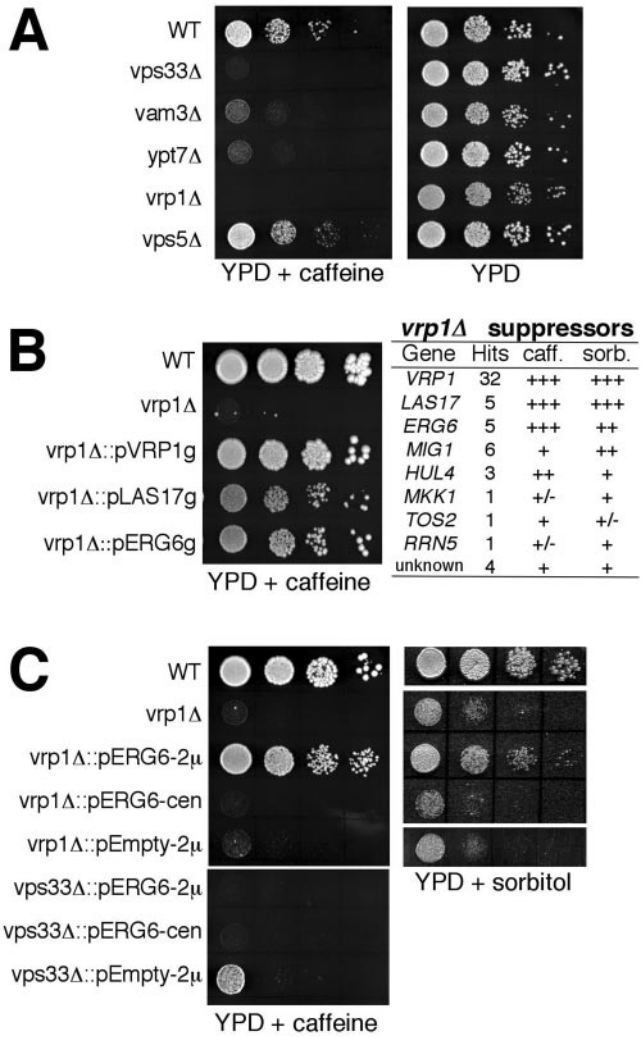

Figure 1. Identification of *ERG6* as a suppressor of the *vrp1*Δ strain. Colony growth assays using a 10-fold dilution series of strains are shown in the BY4742 (WT) background. (A) Addition of 6 mM caffeine to YPD selectively impairs growth of mutants involved in vacuole fusion such as *vam3*Δ (KTY14), *vps33*Δ (KTY11), and *ypt7*Δ (KTY12), but not the *vps5*Δ (KTY13) mutant, which is not involved in fusion. Growth of the actin regulatory mutant, *vrp1*Δ (KTY10), is also impaired on YPD-caffeine. (B) Growth of the *vrp1*Δ mutant is recovered when transformed with a YEp13 genomic library containing the *VRP1*, *LAS17,* or *ERG6* gene (strains KT10-0, 10-40, 10-16, respectively). The table on the right summarizes the suppressor analysis. (C) Transformation with a high-copy plasmid (2μ) containing the *ERG6* opening reading frame rescues growth of the *vrp1*Δ but not *vps33*Δ strains on YPD-caffeine (left panel). Multiple *ERG6* copies also suppress YPD-(1.8 M) sorbitol-sensitive growth (right panel). Transformation with a low-copy plasmid (cen) does not rescue growth.

Vacuole Fusion Reactions

Standard fusion reactions of 30 μl were done in FRB (20 mM PIPES-KOH, pH 6.8, 200 mM sorbitol, 125 mM KCl, 5 mM $MgCl_2$, 10 μM coenzyme A, 6.6 ng/ml leupeptin, 16.6 ng/ml pepstatin, 16.6 μM *o*-phenanthroline, 3.3 μM Pefabloc SC) and 1× ATP (1 mM Mg-ATP, 0.5 mg/ml creatine kinase, 40 mM creatine phosphate). Reactions contained 3 μg of vacuoles isolated from matching genetic strains (see Table 1): one with alkaline phosphatase deleted (*pho8*Δ) and the other with proteinase A and proteinase B deleted (*pep4* Δ, *prb1*Δ), and hence these vacuoles bear inactive proalkaline phosphatase. Reactions were incubated for 90 min at 27°C and then assayed for alkaline phosphatase activity (Haas, 1995). For stimulation of fusion by preincubation with cholesterol, 3 μg of each vacuole pair, from strains KTY1 and 2, or KTY5 and 6, were mixed together with 0–1 mM cholesterol dissolved in 2 mM methyl β-cyclodextrin, and incubated at 4°C, for 45 min in 60 μl of PS buffer (20 nm PIPES-KOH, pH 6.8, 200 mM sorbitol). Vacuoles were then diluted 10-fold in PS buffer, reisolated by centrifugation at 20,000 × *g* for 5 min at 4°C, and resuspended in 30 μl FRB-1× ATP with 0.5 mg/ml cytosol and subjected to standard fusion reaction and assay conditions. Stimulating factors (pure components = IB2, Sec18p, and calmodulin) and inhibiting factors were added as indicated and prepared as previously described (Eitzen *et al.*, 2001, 2002). Cytosol was prepared from strains K91, BY4742, and KTY10 grown to OD_{600} of 4, lysed by vortexing in ice-cold FRB, 2 mM ATP, 1 mM DTT, and 1 volume glass beads for eight 1-min bursts followed by centrifugation at 20,000 × *g*, at 4°C for 20 min. Normally, cytosol from strain K91 was used, which has no endogenous phosphatase activity. However, when examining stimulation of fusion by cytosol devoid of Vrp1p, KTY10 was used and compared with the activity of cytosol prepared from its parental strain BY4742 (see Figure 4, B and C). In these cases cytosol has substantial phosphatase activity and, therefore, was removed by washing vacuoles twice in 0.3 ml 50 mM Tris-Cl, pH 8.5, with centrifugation between washes to precipitate vacuoles. Vrp1p was purified from BY4742 cytosol by ion exchange chromatography using a MonoQ HR 5/5 column and an AKTA Explorer protein purification apparatus (Amersham Bioscience, Piscataway, NJ) and is further described in the legend to Supplemental Figure S2. All fusion values (alkaline phosphatase units) were normalized to the fusion signal from wild-type incubated with 0.5 mg/ml cytosol from four independent experiments to compensate for daily variation in vacuole purification conditions.

Lipid Analysis

Lipids from 200 μg vacuoles were extracted with four volumes of chloroform/methanol (2:1 vol/vol) in the presence of a known amount of tridecanoylglycerol as the internal standard. Polar head groups of phospholipids were digested by phospholipase C (Myher *et al.*, 1989) and free hydroxyl moieties in lipids were derivatized with Sylon BFT (Supelco, Bellefonte, PA). Lipid species were analyzed and quantified by gas chromatography (Agilent Technologies, Wilmington, DE; 6890 Series equipped with a flame ionization detector). Samples were injected onto an Agilent High Performance capillary column (HP-5, 15 m × 0.32 mm × 0.25 μm). The oven temperature was raised from 170 to 290°C at 20°C/min and then to 340°C at 10°C/min with helium as a carrier gas (87 cm/s) with a constant flow rate of 4.5 ml/min. Peak integration is performed with Agilent software. Several close peaks emerge between retention times of 6.1–6.4 min; these represent ergosterol and other yeast sterol intermediates, which were combined to represent total sterols. Likewise, peaks eluting at typical C35–C39 diglyceride retention times were collectively quantified as total phospholipids. The analysis was repeated three times using independent vacuole isolations.

RESULTS

ERG6 Complements Selective Growth Defects in the vrp1Δ Strain

We recently reported a role for actin and its regulatory cascade in vacuole membrane fusion (Eitzen *et al.*, 2002;

Table 2. Primers used in this study

F4-ERG6	5′ tttcattcaagtttcccttatctgttttactttcgagaattcgagctcgtttaaac 3′
R3-ERG6	5′ gaattgggcctgtctttttctcaattctgtttcactgcactgagcagcgtaatctg 3′
5′PEP4-KO	5′ acctagtatttaatccaaataaaattcaaacaaaaaccaaagattgtactgagagtgcac 3′
3′PEP4-KO	5′ tagatggcagaaaaggatagggcggagaagtaagaaaagtctgtgcggtatttcacaccg 3′
5′PHO8-KO	5′ ccagcattacgggacattatttgaacgcgcattagcagcaagattgtactgagagtgcac 3′
3′PHO8-KO	5′ aataaataatatgtgaaaaaagagggagagttagataggactgtgcggtatttcacaccg 3′
5′PRB1-KO	5′ caataaaaaaacaaactaaacctaattctaacaagcaaaagattgtactgagagtgcac 3′
3′PRB1-KO	5′ aagaaaaaaaaaagcagctgaaatttttctaaatgaagactgtgcggtatttcacaccg 3′
5′ERG6	5′ cgggatcccgtttatatagttcgggtgttttctcc 3′
3′ERG6	5′ cgggatcccgttacgatgttgtattcttactatc 3′

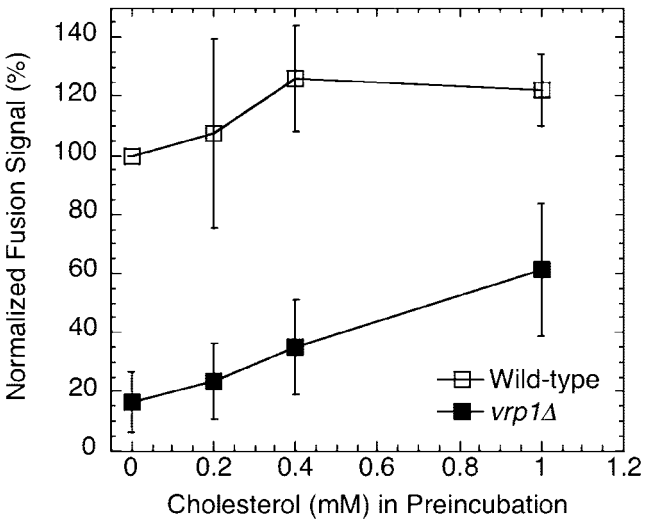

Figure 2. Stimulation of vacuole fusion by preincubation with soluble cholesterol. Vacuoles from the wild-type and *vrp1*Δ strain were preincubated with 0–1 mM cholesterol:2 mM methyl-β-cyclodextrin in 20 mM PIPES, pH 6.8, 200 mM sorbitol for 45 min on ice, reisolated, and resuspended in fusion reaction buffer, 1× ATP and 0.5 mg/ml cytosol. Reactions were incubated for 90 min at 27°C before assaying for alkaline phosphatase. Experiments were repeated four times and normalized to wild-type, 0 mM cholesterol.

Seeley *et al.*, 2002). To further identify factors that may act downstream in the actin pathway, we used a genetic suppressor screen that made use of growth conditions selective for vacuole function. Strains deleted in a number of genes required for vacuole membrane fusion are sensitive to the presence of 6 mM caffeine (Figure 1A) or 1.8 M sorbitol in the medium (our unpublished results; also see Koning *et al.*, 2002). We selected the *VRP1* gene-deletion strains for use in our screen because it also showed sensitive growth under these conditions (Figure 1, B and C) and because it is one of the only genes of the actin regulatory mechanism that is not essential for viability.

The *vrp1*Δ strain was transformed with a multicopy yeast genomic library and transformants were selected for growth on caffeine-containing media. The table in Figure 1B summarizes the result of this suppressor analysis. Most suppressors contained *VRP1* coding sequence as determined by PCR. However 26 transformants grew that did not contain *VRP1* or neighboring sequence. The *LAS17* gene was also a suppressor, which we had anticipated because Las17p is a functional partner of Vrp1p. Las17p and Vrp1p, the yeast homologues of human WASP and WIP, are adapter proteins that link actin assembly and signaling molecules (Evangelista *et al.*, 2000; Higgs and Pollard, 2000). Interestingly, the *ERG6* gene was repeatedly found, and these transformants grew as well as *VRP1* and *LAS17* transformant strains (Figure 1B). Recovery of growth was reconfirmed on media containing 1.8 M sorbitol. Other genes identified rescued growth to a lesser extent and were not studied further because they most likely increased cell viability nonspecifically (i.e., *MIG1*, a transcription factor for RNA pol III; *HUL4*, an E3 ubiquitin protein-ligase; *MKK1*, *TOS2*, and *RRN5* grew poorly).

Genomic library transformants also contained large portions of neighboring sequences (see Table 1). To confirm that the *ERG6* gene caused the suppression phenotype, it was subcloned into multicopy (pRS425) and single copy (pRS315) plasmids. The subcloned *ERG6* gene also gave a suppression phenotype that was dependent on multiple copies. *ERG6* expression from a single-copy plasmid (*cen*) did not recover growth (Figure 1C). *ERG6* suppression was also specific for the *vrp1*Δ strain because transformation of another vacuole fusion mutant, *vps33*Δ, was not rescued (Figure 1C).

Cholesterol Partially Restores Fusion of vrp1Δ Vacuoles

A complete ergosterol synthesis pathway is needed for vacuole assembly in vivo, whereas exogenously added ergosterol (or cholesterol) can partially restore vacuole fusion in vitro in the absence of ergosterol synthesis (Kato and Wickner, 2001). Vacuole assembly is defective in the *vrp1*Δ strain (Eitzen *et al.*, 2002) and purified vacuoles do not fuse in vitro (see Figure 4A, *vrp1*Δ *vacuoles*, lane "none"). When *vrp1*Δ vacuoles were preincubated with increasing amounts of methyl-β-cyclodextrin solubilized cholesterol, a small but consistent increase in fusion signal was obtained (Figure 2). Addition of similar amounts of cholesterol to vacuoles from the wild-type strain stimulated fusion only slightly at low concentrations. These results taken together with *ERG6* suppression of *vrp1*Δ growth defect, suggested that lipids play a vital role in the actin regulation of membrane fusion and that local increases in sterols may provide a means to bypass the need for Vrp1p in vacuole biogenesis.

ERG6 Overexpression Enhances Vacuole Fusion

We next constructed several strains that endogenously overexpressed *ERG6* as an alternative approach to manipulate sterol levels in vivo, and then we examined the effect on the fusion of isolated vacuoles. To do this the *GAL1* promoter (P_{GAL1-}) and three heamagglutinin antigen (HA) epitopes were inserted in front of the genomic *ERG6* copy. Up to 12-fold enhanced synthesis of Erg6p was achieved when these cells were grown in galactose-containing media compared with dextrose (Figure 3A). Using a mixture of both dextrose and galactose also resulted in a large increase (about fivefold) in Erg6p levels (Figure 3A, second lane). Growth curves were generated for *ERG6* overexpression and parental strains using YP media containing either 2%

Table 3. Percentage of nonextractable vacuolar membrane proteins

		Extraction Buffer	
Strain	Genotype	50 mM Tris-Cl, pH 8.5	100 mM Na_2CO_3, pH 11.5
KTY1	Wild-type	73.2% ± 8.8%	37.5% ± 6.2%
KTY3	Wild-type P_{GAL1}-*ERG6*	75.5% ± 5.2%	46.2% ± 3.1%
KTY5	*vrp1*Δ	71.6% ± 6.4%	42.1% ± 4.4%
KTY7	*vrp1*Δ P_{GAL1}-*ERG6*	73.8% ± 5.9%	54.7% ± 3.6%

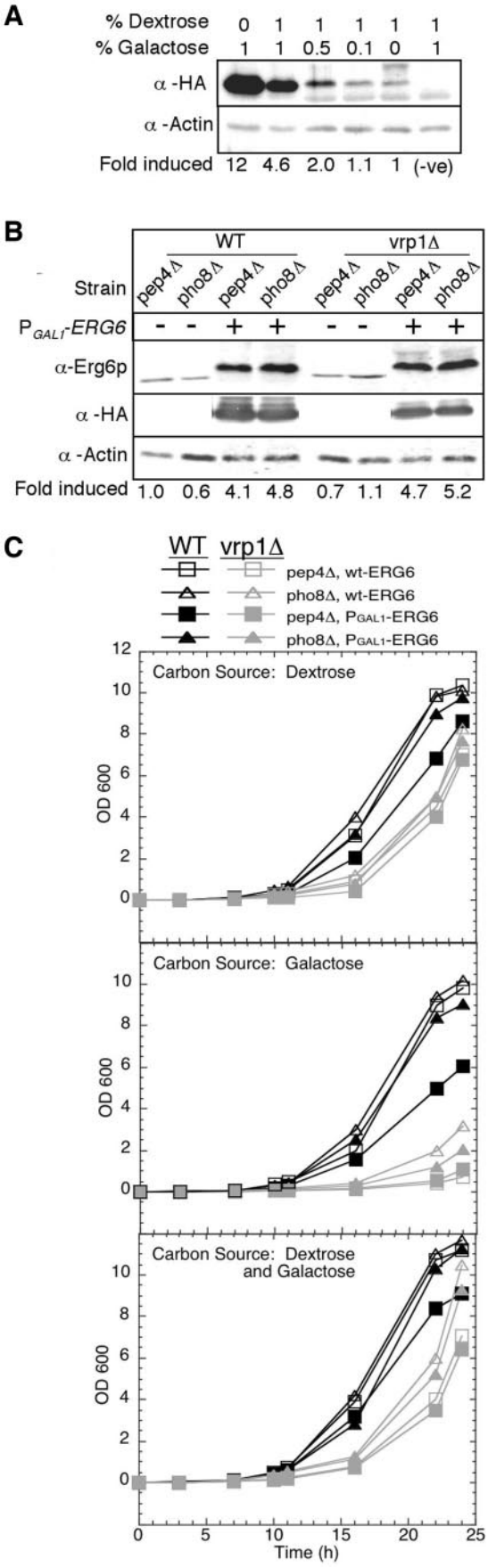

dextrose, 2% galactose, or 1% of each. The results showed a significant reduction in growth rates, especially for the *vrp1*Δ strains, when galactose was the sole carbon source (Figure 3C, middle panel). Media with 1% dextrose and 1% galactose restored healthy growth rates (Figure 3C, bottom panel) and showed significant increases in Erg6p production (Figure 3B). These conditions were subsequently used to grow cells for the production of vacuoles to be used in fusion reactions.

Vacuoles isolated from strains overexpressing *ERG6* showed large increases in in vitro fusion (Figure 4A, WT vacuoles). Vacuoles isolated from the *vrp1*Δ strain did not undergo in vitro fusion, but overexpression of *ERG6* before vacuole isolation rescued this defect (Figure 4A, *vrp1*Δ vacuoles, compare gray bars with hatched bars). Common membrane fusion inhibitors such as calcium chelators (BAPTA) and antibodies to NSF/Sec18p (our unpublished results) and SNAREs (anti-Vam3, the vacuolar t-SNARE) efficiently blocked these reactions, showing that the normal fusion pathway is followed. A second observation we made was that higher concentrations of cytosol were needed to maximally stimulate fusion in reactions with vacuoles from the *vrp1*Δ strain (Supplementary Figure S1A, compare solid triangles with boxes). Pure components (PC), which normally stimulate fusion, were ineffective at stimulating fusion in the absence of Vrp1p (Figure 4A, *vrp1*Δ background, compare PC bars to cytosol bars). This indicated the need for additional cytosolic components in *vrp1*Δ backgrounds and suggests that deletion of *VRP1* may cause aberrant protein processing or localization.

To test if the cytosol stimulation of *vrp1*Δ vacuoles simply reflects the resupplying of Vrp1p, we made cytosol from the *vrp1*Δ strain. In a direct comparison with wild-type cytosol, *vrp1*Δ cytosol supported fusion to a similar level (Figure 4, B and C). *vrp1*Δ cytosol titration resulted in similar stimulation curves as previously observed with wild-type cytosol (Supplementary Figure S1B). To directly test if Vrp1p affects fusion, a semi-purified fraction was isolated (see Supplementary Figure S2). Readdition of Vrp1p alone had no affect on the fusion of wild-type vacuoles, although slightly enhanced fusion when *ERG6* was overexpressed (Figure 4B, compare gray bars within data sets). Readdition of Vrp1p, alone or with cytosol, could not recover fusion of vacuoles

Figure 3. Characterization of *ERG6* overexpression strains. The galactose-regulated *GAL1* promoter and three HA epitopes were introduced inframe at the 5′ end of the *ERG6* gene. (A) Expression of P_{GAL1}-HA-*ERG6* was examined 24 h after inoculating 10 ml of YP media with varying dextrose:galactose ratios from a single YPD preculture of strain KTY3. Strain KTY1 was included as a negative control (no P_{GAL1}-HA-*ERG6* allele). Equivalent culture volumes were processed for immunoblot analysis with anti-HA and anti-actin as a load control. Bands were analyzed by densitometry and normalized to 1% dextrose to calculate fold induced. (B) Erg6p expression levels were examined in cultures grown in YP 1% dextrose/1% galactose to 1 OD_{600} for vacuole isolation. Culture equivalents of 0.25 OD_{600} units were processed from strains with P_{GAL1}-HA-*ERG6* induction, KTY3-4 (WT) and KTY7-8 (*vrp1*Δ), and from cultures without P_{GAL1}-HA-*ERG6,* KTY1-2 (WT) and KTY5-6 (*vrp1*Δ). Immunoblot analysis was performed with both anti-Erg6p (gift from G. Daum) and anti-HA for direct comparison. Anti-Erg6p bands were analyzed by densitometry and normalized to wild-type *pep4*Δ (KTY1). (C) Growth curves were generated for wild-type (strains KTY1-4) and *vrp1*Δ mutants (strains KTY5-8) by inoculating 0.1 ml of 1 OD_{600} cultures into 50 ml of fresh YP media containing either 2% dextrose (top panel), 2% galactose (middle panel), or 1% dextrose/1% galactose (bottom panel).

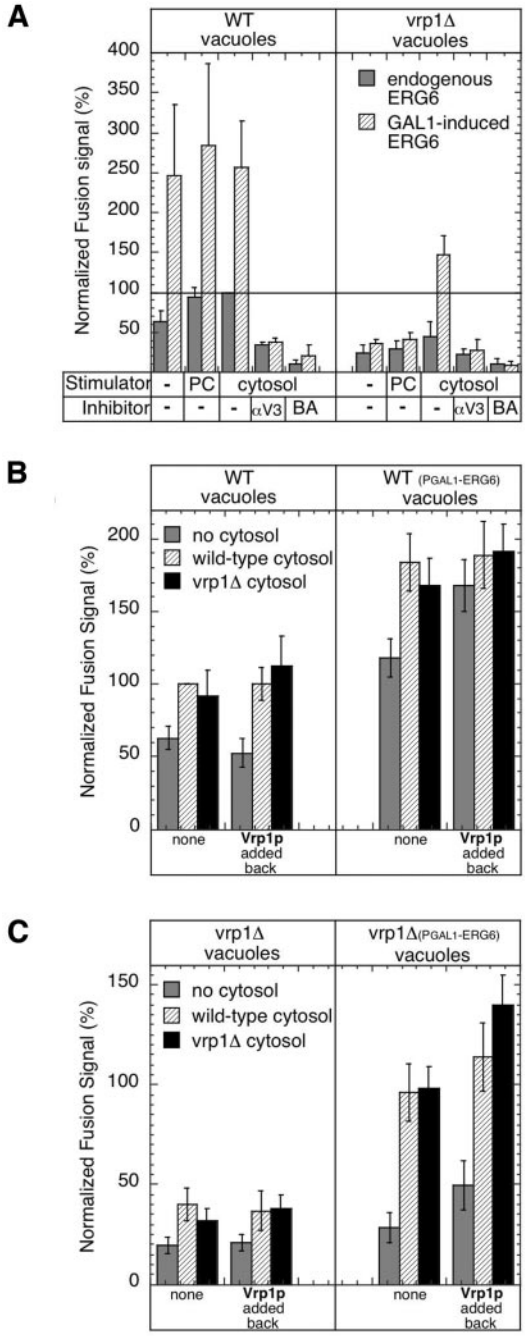

Figure 4. Stimulation of vacuole membrane fusion by *ERG6* overexpression. (A) Fusion reactions using vacuole pairs isolated from strains KTY1 and 2 (WT vacuoles, gray bars) or KTY5 and 6 (*vrp1*Δ vacuoles, gray bars), and with P_{GAL1}-*ERG6* induction from strains KTY3 and 4 (WT vacuoles, hatched bars) or KTY7 and 8 (*vrp1*Δ vacuoles, hatched bars). Stimulators of fusion added to reactions were optimized amounts of cytosol (cytosol) as in Supplementary Figure S1A, or pure components (PC, 200 μg/ml calmodulin, 8 μg/ml IB2, 1 μg/ml Sec18p). Inhibitors of fusion added to reactions were anti-Vam3p IgG (150 μg/ml) or 3 mM BAPTA. (B and C) Cytosol/Vrp1p stimulation of vacuole fusion. Reactions were incubated without cytosol (gray bars) or with 0.5 mg/ml cytosol prepared from wild-type strain (hatched bars) or *vrp1*Δ strain (black bars) strains using vacuole pairs from wild-type (B) and *vrp1*Δ (C) genetic backgrounds as in panel A. Stimulation was examined in identical reactions supplemented with 20 μg/ml semi-purified Vrp1p (Vrp1p, added back) or without this addition (none). See Supplementary Figure S2 for a description of Vrp1p preparation.

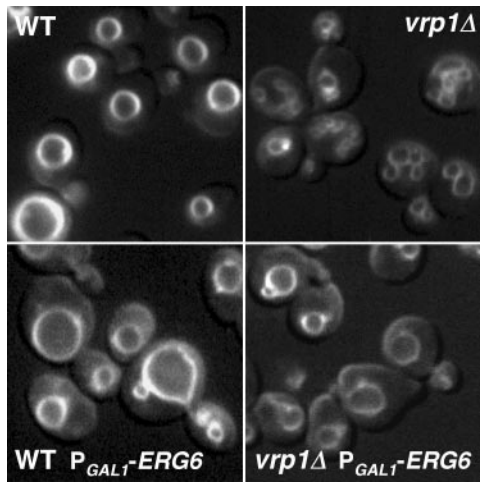

Figure 5. *ERG6* overexpression recovers normal vacuole morphology in *vrp1*Δ strains. FM4–64 staining of vacuoles in WT and *vrp1*Δ backgrounds (top panels, KTY1 and KTY5) and similar strains bearing the P_{GAL1}-*ERG6* allele (bottom panels, KTY3 and KTY7). Growth media contained 1% dextrose/1% galactose in all cases.

from the *vrp1*Δ strain (Figure 4C, left panel). However when vacuoles were isolated from the *vrp1*Δ-*ERG6* overexpression strain, readdition of Vrp1p boosted fusion signals, especially in the presence of *vrp1*Δ cytosol (Figure 4C, right panel, compare black bars). In all cases, fusion was blocked when Vam3p antibodies were present in reaction mixtures (our unpublished results), maintaining that the reaction mechanism catalyzed by Vrp1p and bypassed by *ERG6* is connected to the normal SNARE-mediated fusion pathway.

ERG6 overexpression also rescued vacuole fusion in vivo as judged by vacuole morphology. Vacuoles were stained in live wild-type and *vrp1*Δ mutant cells with the vital dye FM4-64. Normal morphology is one to three large vacuoles per cell, which was seen in wild-type cells regardless of P_{GAL1}-*ERG6* induction (Figure 5, left panels). Fragmented vacuoles were observed in *vrp1*Δ mutant cells (Figure 5, top right panel); however, when P_{GAL1}-*ERG6* was introduced and induced, this fragmented morphology was clearly reduced and a more normal vacuole morphology arose (Figure 5, bottom right panel). Therefore, in vivo vacuole assembly is also rescued by *ERG6* overexpression.

ERG6 Overexpression Also Bypasses the Need for Las17p But Not Actin Remodeling

To further characterize whether components of the actin-regulated fusion mechanism downstream of Vrp1p are bypassed by *ERG6* overexpression, several additional actin inhibitors were tested (Eitzen *et al.*, 2002). The drugs latrunculin B and jasplakinolide, which block actin remodeling, remain active inhibitors of fusion regardless of the vacuole source (Figure 6). However, Las17p antibodies, which are active fusion inhibitors of wild-type vacuoles (Figure 6A, left panel), showed reduced inhibition when vacuoles were isolated from the wild-type–*ERG6* overexpression strains (Figure 6A, right panel) and no inhibition when vacuoles were isolated from *vrp1*Δ–*ERG6* overexpression strains (Figure 6B, right panel). To confirm these results, the growth suppression analysis was retested with the *las17-16* conditional mutant strain (DDY2266, Duncan *et al.*, 2001). This strain shows fragmented vacuole morphology (Eitzen *et al.*, 2002) and does not accumulate the red colored *ade2* fluorophor,

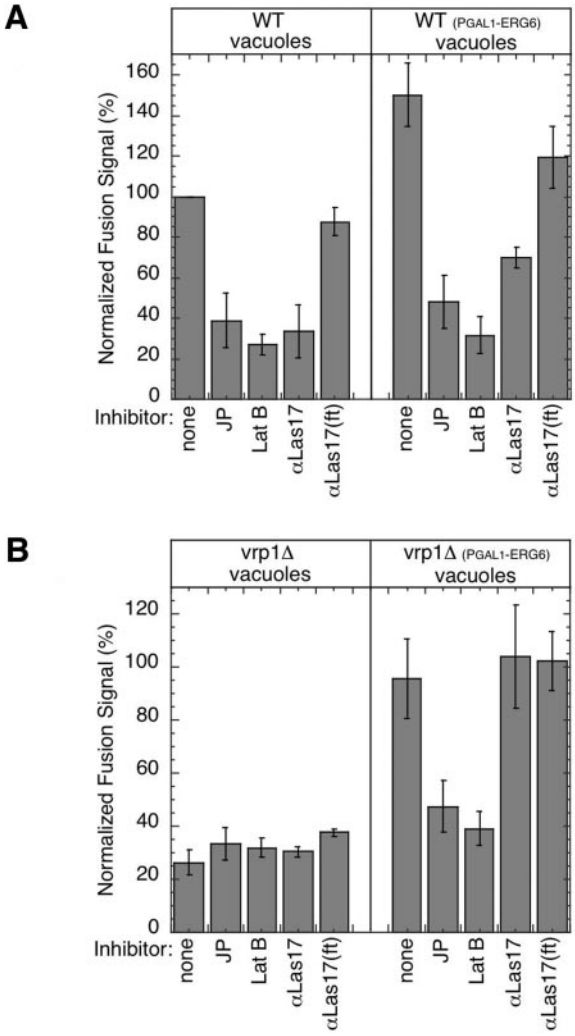

Figure 6. *ERG6* induction bypasses Las17p antibody inhibition but actin ligand inhibition is maintained. (A) Standard fusion reactions with wild-type vacuoles (right panel, strains KTY1 and 2) or wild-type sterol-enriched vacuoles (left panel, strains KTY3 and 4) were incubated with 0.2 mM jasplakinolide (JP), 0.4 mM latrunculin B, 250 μg/ml Las17p antibodies, or Las17p antibodies adsorbed to DEAE-sepharose (αLas17(ft)). (B) Standard fusion reactions as in A, except *vrp1*Δ vacuoles (right panel, strains KTY5 and 6) or *vrp1*Δ sterol-enriched vacuoles (left panel, strains KTY7 and 8) were used.

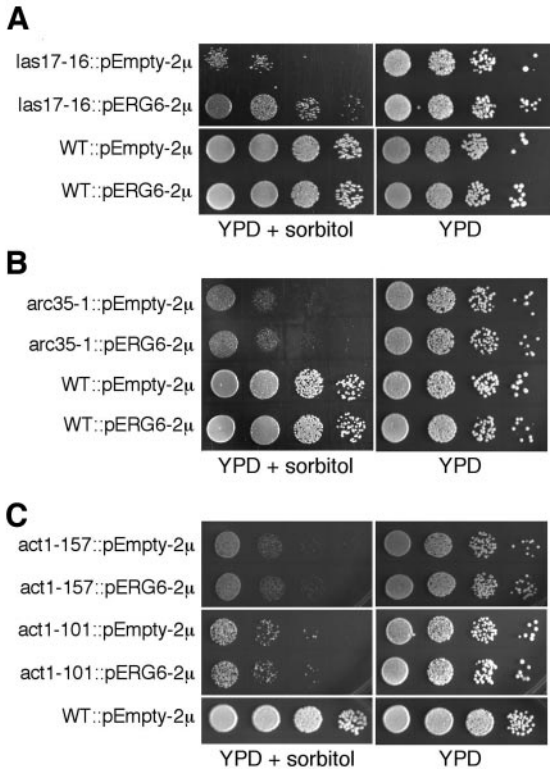

Figure 7. *ERG6* suppresses a specific growth defect of the *las17-16* mutant, but not that of other mutants downstream of Vrp1p/Las17p. Colony growth assays using a 10-fold dilution series of cultures are shown with their respective parental (WT) and mutant backgrounds (see Table 1). Addition of 1.8 M sorbitol to YPD selectively impairs the growth of mutants involved in vacuole biogenesis (Koning *et al.*, 2002) as well as the actin-remodeling mutants *las17-16* (A), *arc35-1* (B), and the direct actin mutants *act1-157* and *act1-101* (C). Transformation with the *ERG6* gene on a multicopy plasmid (*pERG6–2*μ) restores growth of the *las17-16* mutant (A), but has no effect on the other mutants (B and C).

which accumulates in vacuoles of the parental strain (DDY2246) and is indicative of a vacuole assembly defect (Weisman *et al.*, 1987). The *LAS17* parental strain was slightly sensitive to 6 mM caffeine, and therefore the suppressor analysis was done using 1.8 M sorbitol. Under these conditions the *las17-16* strain was significantly more sensitive than its parental strain (Figure 7A, *pEmpty-2*μ*)*. This growth defect was suppressed when *las17-16* was transformed with a high-copy plasmid bearing the *ERG6* gene (Figure 7A, *pERG6–2*μ*)*. Together these results maintain that the actin regulatory step controlled by the Las17p/Vrp1p complex is completely bypassed by *ERG6*.

Using the same analysis, we tested several other actin regulatory mutants downstream of Las17p/Vrp1p to determine how far in the actin-remodeling pathway *ERG6* suppression extends. Arc35p is an essential component of the Arp2/3 complex, which is immediately downstream of Las17p/Vrp1p (Schaerer-Brodbeck and Riezman, 2000). The *arc35-1* mutant showed sorbitol-sensitive growth that was not recovered by *ERG6* overexpression (Figure 7B). As well the actin mutants, *act1-101* and *act1-157*, showed retarded growth under similar conditions that was not suppressed by *ERG6* overexpression (Figure 7C). This is in accord with the maintenance of actin ligand sensitivity in fusion reactions (Figure 6). Therefore, post-Vrp1p/Las17p steps of actin regulation are not suppressed by *ERG6*.

VRP1 Deletion Affects Vacuolar Sorting, which Is Not Altered by ERG6 Overexpression

To try and further define why increased *ERG6* expression stimulates vacuole fusion and resurrects fusion-dead vacuoles from the *vrp1*Δ strain, vacuolar protein sorting was examined. We observed a greater cytosolic dependence in fusion reactions when using vacuoles from the *vrp1*Δ strain (Figure 4C), which suggested a protein localization defect. Rescue of a sorting defect as previously indicated from the inability of PC to support fusion (see explanation for Figure 4A) or creating a more efficient sorting environment would be a plausible explanation as to why elevated *ERG6* stimulates fusion.

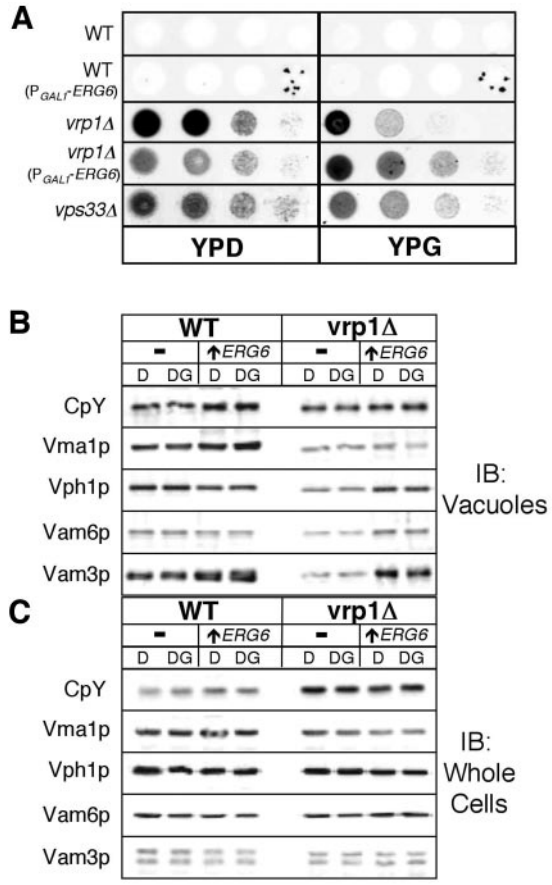

Figure 8. *ERG6* induction does not rescue *vrp1*Δ sorting defects. (A) Secretion filter binding assays showing the relative extracellular levels of the vacuole luminal protein, CpY, in wild-type and *vrp1*Δ strains, both without (YPD) and with (YPG) P_{GAL1}-*ERG6* induction. A 10-fold dilution series of the indicated strains were plated, filters were overlaid, and incubated for 48 h at 28°C before immunoblot analysis. The vacuolar protein sorting mutant, *vps33*Δ, is shown for comparison. (B and C) Equal cellular fraction of vacuoles (B) and whole cells (C) were analyzed by SDS-PAGE and immunoblotting. Samples were prepared from the WT strain KTY1 (−), WT with the P_{GAL1}-*ERG6* allele KTY3 (↑ *ERG6*), *vrp1*Δ strain KTY5 (−), and *vrp1*Δ with the P_{GAL1}-*ERG6* allele KTY7 (↑ *ERG6*). Growth condition were YP with either 2% glucose (D) or 1% glucose/1% galactose (DG) to induce P_{GAL1}-*ERG6* expression.

To characterize whether *VRP1* deletion and upregulation of *ERG6* affects vacuolar protein sorting, we examined if CpY, a vacuolar luminal protein, was missorted to the plasma membrane by filter binding assays (Roberts *et al.*, 1991). Starting with cultures at 1 OD_{600}, a 10-fold dilution series was plated onto YP-agar with either 2% dextrose or 1% galactose/0.2% dextrose to induce *ERG6* expression. Filters were applied and incubated for 48 h at 28°C. Immunoblot analysis showed that CpY was found extracellularly in the *vrp1*Δ strain, regardless of P_{GAL1}-*ERG6* induction (Figure 8A, compare YPD with YPG). This is similar to the *vps33*Δ strain (Figure 8A), which is know to secrete vacuolar proteins. Whole cell and vacuolar levels of CpY and several other vacuolar proteins were also examined in cells similarly grown to 1 OD_{600} by SDS-PAGE and immunoblot. No change was observed in whole cell levels, regardless of P_{GAL1}-*ERG6* induction (Figure 8C). The vacuolar levels of several proteins were reduced in the *vrp1*Δ background. The V-ATPase subunits Vma1p and Vph1p, the t-SNARE Vam3p, and the tethering factor Vam6p, were all reduced in vacuoles from the *vrp1*Δ strain. Wild-type levels of all proteins except Vma1p were restored in vacuoles from the *vrp1*Δ strain that contained the P_{GAL1}-*ERG6* allele, though this recovery was independent of *ERG6* induction (Figure 8B, compare column D with DG). These results do not support a hypothesis that *ERG6* overexpression corrects sorting defects because we observed little effect on sorting in the *vrp1*Δ strain when directly comparing results from induced and uninduced cultures.

ERG6 induction caused an increase in the levels of the membrane protein Vam3p and, to lesser extent, Vph1p, especially in the *vrp1*Δ background (Figure 8B). We therefore examined the relative proportion of membrane-bound and integral membrane proteins by extraction with 50 mM Tris-Cl, pH 8.5, and 100 mM Na_2CO_3, pH 11.5, respectively. Immunoblot was used to determine extraction efficiency. The membrane marker Vph1p was localized to the membrane pellet fraction and the luminal marker CpY was localized to the soluble fraction after each treatment; whereas the peripheral membrane protein, Vam6p, was only completely extracted by Na_2CO_3 treatment (Supplementary Figure S3). Table 3 shows that the wild-type strain bearing an inducible *ERG6* gene has slightly increased levels of vacuolar integral membrane proteins, which is further augmented by deletion of *VRP1*. Hence, the increase in vacuolar membrane proteins seen on immunoblots (Figure 8B) reflects the rise in the relative proportion of vacuolar integral membrane proteins by *ERG6* induction.

Modification of Vacuolar Lipids via ERG6 Induction

We next tested whether elevated *ERG6* expression changed the vacuolar lipid environment. This in turn could produce a more favorable environment for the membrane fusion machinery to function. Vacuoles were isolated from the wild-type and *vrp1*Δ strain, both with and without P_{GAL1}-

Table 4. Quantification of lipids from purified vacuoles (mg/mg protein)

Strain	Genotype	Total sterols	Sterols fold inc.	Total phospholipids	Sterols:Phospholipid	Sterol esters
KTY1	Wild-type	0.25 ± 0.021	1.00	0.98 ± 0.024	0.26	0.14 ± 0.013
KTY3	Wt P_{GAL1}-*ERG6*	0.36 ± 0.018	1.44	0.92 ± 0.058	0.39	0.27 ± 0.012
KTY5	*vrp1*Δ	0.26 ± 0.015	1.04	0.98 ± 0.081	0.27	0.24 ± 0.007
KTY7	*vrp1*Δ P_{GAL1}-*ERG6*	0.39 ± 0.010	1.56	0.94 ± 0.010	0.41	0.34 ± 0.021

Cells were grow in YP media with 1% dextrose/1% galactose as the carbon source. Vacuoles were isolated from cultures grown overnight to 1 OD_{600}. Vacuolar protein concentrations were determined, and 200 μg of each were pelleted by centrifugation before use in this assay.

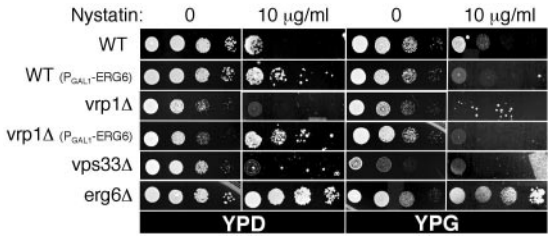

Figure 9. *ERG6* induction increases nystatin sensitivity. (A) Colony growth assays to test the sensitivity of strains to 10 μg/ml nystatin, indicative of increased levels of ergosterol. A 10-fold dilution series of the indicated strains were plated on YP media with 2% dextrose (YPD) or 1% galactose/0.2% dextrose (YPG). Growth was examined after 2 d in the absence of nystatin and 4 d in the presence of nystatin.

ERG6 induction. Lipids were extracted from equal amounts of vacuoles based on protein with chloroform:methanol and quantified by gas chromatography. Normally, ergosterol elutes as a single peak; however, in our analysis all vacuole lipid profiles showed multiple peaks near the ergosterol retention time, representing ergosterol and an assortment of intermediates of ergosterol synthesis (our unpublished observations). These peaks were collectively quantified as total sterols; likewise, all peaks representing different phospholipids were collectively quantified as total phospholipids (Table 4). The *ERG6* overexpression strain KTY3, showed an ~1.5-fold increase in vacuolar sterol levels compared with vacuole lipids from the parental strains KTY1, based on equivalent vacuolar protein. Similar results were obtained from vacuoles prepared from the *vrp1*Δ mutant strain (see Table 4, strains KTY5 and KTY7 for *vrp1*Δ with and without *ERG6* overexpression, respectively). In the same analysis phospholipid levels did not show significant increases due to *ERG6* induction. Hence there is an overall rise in the sterol:phospholipid ratio indicative of sterol enrichment within vacuole membranes due to *ERG6* overexpression. Sterol esters were also increased ~1.6-fold by induction of *ERG6* expression. Esters are generally considered a storage form of lipids that are rapidly available when needed and thus may also be a contributing factor. Interestingly, sterol ester levels were consistently higher in the *vrp1*Δ strain vacuoles; we speculate this is partly due to the mild sorting defect of these strains.

A second way to examine sterol levels is sensitivity to the drug nystatin. Yeast growth is resistant to nystatin when ergosterol synthesis is compromised and hypersensitive when ergosterol levels are increased (Parks *et al.*, 1999). Colony growth assays were used to examine strain sensitivity to media containing 10 μg/ml nystatin as a secondary indicator of ergosterol levels. Increased resistance to nystatin was observed in deletion strains of the ergosterol synthesis pathway as expected (Figure 9, compare *erg6*Δ with WT), or when expression of P_{GAL1}-*ERG6* was repressed on dextrose (Figure 9, *WT* (P_{GAL1}-*ERG6*), compare YPD with YPG). Strains with defects in vacuole biogenesis showed increased nystatin sensitivity (Figure 9, compare *vps33*Δ and *vrp1*Δ with WT). Sensitivity to nystatin consistently increased in strains with P_{GAL1}-*ERG6* induction. This supports the conclusion that *ERG6* overexpression causes a rise in ergosterol levels. In addition, the *vrp1*Δ strain bearing the P_{GAL1}-*ERG6* allele became resistant to nystatin when expression was repressed on dextrose (Figure 9, *vrp1*Δ (P_{GAL1}-*ERG6*), compare YPD with YPG). This indicates that reduced ergosterol levels may be an overriding factor to vacuolar biogenesis defects when examining nystatin sensitivity. Alternatively, *vps* mutants may be nystatin sensitive because of increased plasma membrane sorting, causing an effective rise in ergosterol levels.

We next examined if this altered lipid environment can promote the function of the membrane fusion machinery. Membrane fusion kinetics were examined by removing aliquots of standard fusion reactions to ice at various times. These results showed peak fusion values were achieved when reactions contained vacuoles isolated from strains bearing the P_{GAL1}-*ERG6* allele, whereas wild-type vacuoles did not reach maximum values in the time course of this experiment (Figure 10A, top panel). Instantaneous fusion kinetics were calculated as the change in alkaline phosphatase units vs. time averaged over 30 min. This analysis showed that the increase in fusion is primarily due to an increase in the rate at early time points (Figure 10A, bottom panel). To initiate membrane fusion vacuoles undergo priming, a process requiring ATP hydrolysis by Sec18p and the release of Sec17p (Mayer *et al.*, 1996). Because the difference in fusion rates were most dramatic at early time points, we examined if priming kinetics were altered because of *ERG6* induction. Approximately 33% of vacuolar-bound Sec17p is released from wild-type vacuoles by 10 min; this is increase to 90% by 30 min after which little change is observed (Figure 10B). Induction of *ERG6* caused an increase in both the kinetics of Sec17p release with 56 and 79% released by 5 and 10 min, respectively, and a final level of near-complete release was achieved by 30 min. Deletion of the *ERG6* gene reduced the rate and level of Sec17p release (Figure 10D). In the *vrp1*Δ strain little release of Sec17p was observed; introduction and induction of the P_{GAL1}-*ERG6* allele recovered this activity (Figure 10C). This data supports a hypothesis that the altered lipid environment due to *ERG6* induction promotes the activity of the membrane fusion machinery specifically during the priming subreaction.

Actin Remodeling during Vacuole Fusion

Actin associates with vacuoles and is remodeled during fusion and an early subreaction is sensitive to filamentous actin stabilization (Eitzen *et al.*, 2002). Vrp1p is known to be part of the actin remodeling machinery (Evangelista *et al.*, 2000); thus we wanted to link actin-related defects on vacuoles isolated from the *vrp1*Δ strain to compensation via sterol enrichment. We assayed actin turnover by examining the levels that remain vacuole associated during fusion reactions without cytosol to limit the amount of rebinding. Actin was slowly shed from wild-type vacuoles during these reactions, and this activity was augmented by sterol enrichment via *ERG6* induction (Figure 11, A and B, compare WT with WT P_{GAL1}-*ERG6*). Deletion of *VRP1* reduced actin shedding activity, whereas induction of *ERG6* in the *vrp1*Δ background recovered actin release (Figure 11, A and B, compare *vrp1*Δ with *vrp1*Δ P_{GAL1}-*ERG6*). This subreaction is driven by an ATPase activity because apyrase inhibits actin release (Figure 11B). However, it is different from the subreaction involving Sec17p because actin release is not affected by incubation with Sec17p antibodies (Figure 11B). As well the time-frame and extent of release differs from Sec17p release and would place actin shedding into the docking subreaction in accord with jasplakinolide inhibition (Wickner, 2002). Therefore the efficiency of both priming and docking subreactions are affected by lipid compositions.

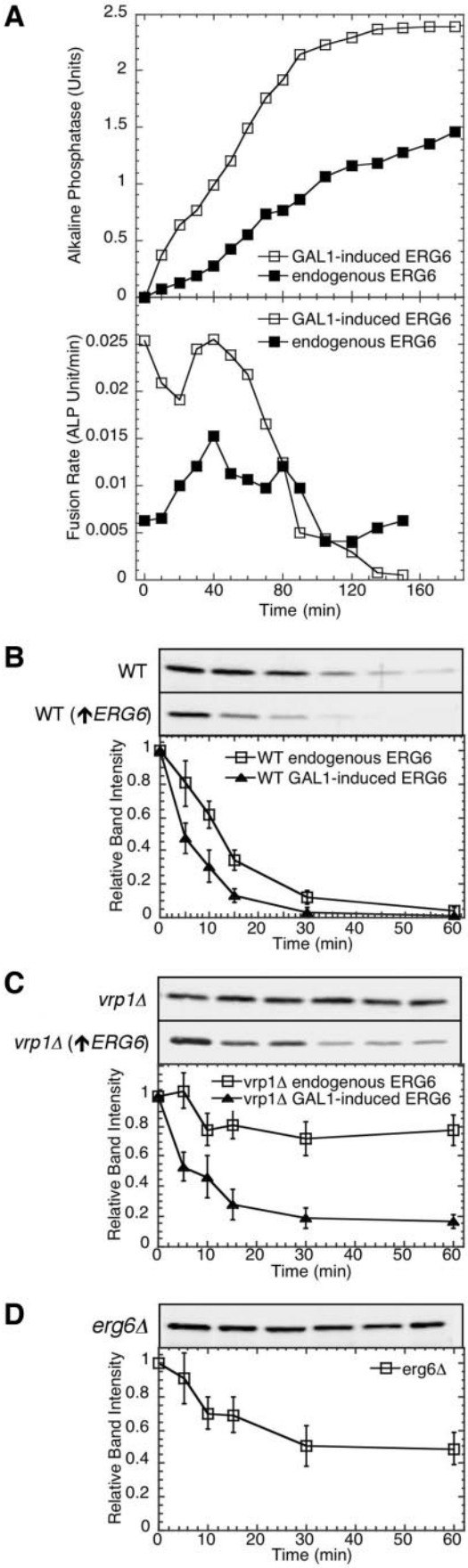

DISCUSSION

Recently we reported a membrane fusion regulatory mechanism that involved signaling through Rho proteins to actin (Eitzen *et al.*, 2002). Inhibition of actin dynamics with specific drugs caused a differential effect on in vitro vacuole membrane fusion. Blocking actin depolymerization affected only vacuole docking, whereas blocking actin polymerization affected bilayer fusion. To learn more about the actin-regulated steps of vacuole fusion, we devised a multicopy suppressor screen using mutant strains within the pathway from Rho proteins to actin (Eitzen, 2003). We would have preferred to perform this screen with the Rho mutants *cdc42-1* and *rho1-104*, which are defective for vacuole fusion (Eitzen *et al.*, 2001; Müller *et al.*, 2001). However, these strains were prone to genetic reversion, likely due to the presence of semi-functional Rho proteins. Therefore, we used the *vrp1*Δ strain because this was the only gene in the actin regulatory pathway that could be deleted and still produce strains with acceptable growth rates. Vrp1p is localized to the vacuole and was independently found to physically interact with the vacuolar Rab, Ypt7p, and V-ATPase subunit, Vma1p (Eitzen *et al.*, 2002; Gavin *et al.*, 2002). Vacuoles isolated from the *vrp1*Δ strain do not fuse in vitro (Figure 4A) and are fragmented in vivo (Figure 5), which supports a role for Vrp1p in vacuole membrane fusion. Deletion of *VRP1* led to sorbitol- and caffeine-sensitive growth (Figure 1), which also supports a role for Vrp1p in vacuole biogenesis because these conditions have previously been shown to impair the growth of vacuole biogenesis mutants that are involved in homotypic fusion (Kucharczyk *et al.*, 2000; Koning *et al.*, 2002).

Here we report a specific genetic interaction between *VRP1* and *ERG6*. *ERG6* was isolated as a multicopy suppressor of caffeine- and sorbitol-sensitive growth of the *vrp1*Δ strain (Figure 1). *ERG6* rescued *vrp1*Δ growth as efficiently as the wild-type *VRP1* gene, but did not rescue *vps33*Δ, a mutant also defective for vacuole fusion. This rules out the possibility that *ERG6* overexpression nonspecifically increases cell viability on caffeine or sorbitol media. *ERG6* induction also suppressed similar growth defects of a *las17* conditional mutant (Figure 7A). *ERG6* suppression was limited to *vrp1*Δ and *las17* mutants, because downstream mutants were not rescued for growth (Figure 7, B and C).

Oversynthesis of the *ERG6* gene from the *GAL1* promoter in the *vrp1*Δ strain rescued vacuole fusion in vitro, and recovered normal vacuole morphology in vivo (Figures 4A and 5). This rescue effect was completely dependent on the addition of cytosol, whereas previously characterized solu-

Figure 10. Enhanced membrane fusion and priming kinetics via *ERG6* induction. (A) Standard fusion reactions contained wild-type vacuoles from strains KTY1 and 2, or wild-type sterol-enriched vacuoles from strains KTY3 and 4. At various times aliquots were placed on ice to stop further fusion. Reactions were then assayed for alkaline phosphatase activity (top panel), and the rate of fusion was calculated as follows: ALP units$_{(tn\ +\ 30\ min)}$ − ALP units$_{(tn)}$/time (bottom panel). (B and C) Fusion reactions, supplemented with 5 μg/ml Sec18p, were analyzed for Sec17p release by coprecipitation with vacuoles. Immunoblots show the decrease of membrane-bound levels of Sec17p over time (0, 5, 10, 15, 30, and 60 min). Vacuoles were prepared from wild-type (B) and *vrp1*Δ (C) strains either with sterol enrichment via P_{GAL1}-*ERG6* induction (▲) or without (□). (D) Sec17p release from vacuoles isolated from the *erg6*Δ strain (KTY15). Immunoblots from four experiments were analyzed by densitometry (see *Materials and Methods*), and values were normalized to maximum signals. Error bars, SE.

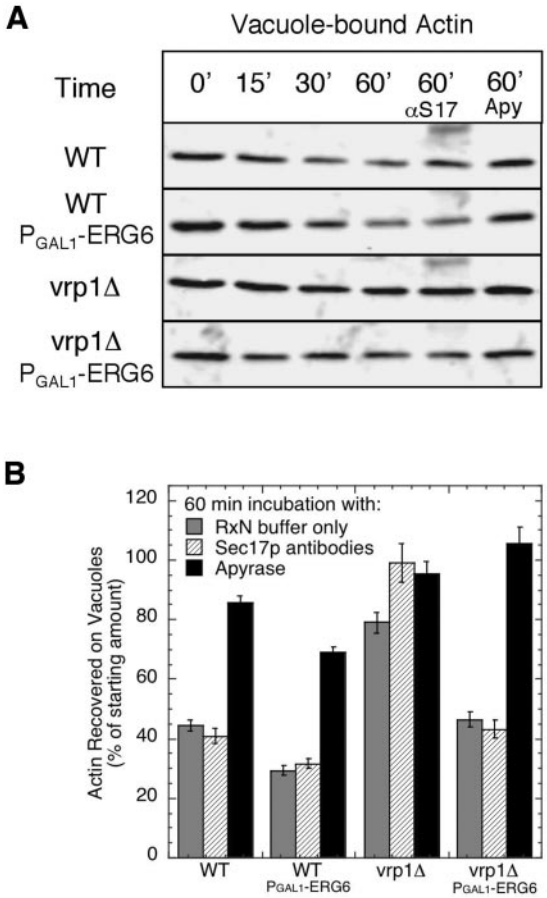

Figure 11. Release of vacuole-associated actin requires ATP and Vrp1p. Standard fusion reactions were analyzed for bound actin by coprecipitation with vacuoles and immunoblot analysis. At the specified times, reactions were stopped by fivefold dilution on ice and immediate centrifugation to precipitate vacuoles and associated proteins. Changes in vacuole-associated actin were determined by densiometric analysis of immunoblots. (A) Immunoblots showing typical actin reduction using vacuoles from wild-type and *vrp1*Δ strains, either with (P_{GAL1}-*ERG6*) or without sterol enrichment. Actin release activity is not blocked by incubation with 250 μg/ml Sec17p antibodies (αS17) but is block by addition of 0.025 U/ml apyrase VII (Apy). (B) Quantification of release activity by analysis of vacuole-associated actin remaining after 60 min using reactions as in panel A. Immunoblots from five experiments were analyzed by densitometry (see *Materials and Methods*), and values represent the average reduction of vacuole-associated actin using 0 min as 100% for each data set. Error bars, SE.

ble fusogens (Sec18p, IB2, calmodulin) could not stimulate fusion (Figure 4A). To test whether Vrp1p is a component of cytosol contributing to membrane fusion, cytosol was prepared from the *vrp1*Δ strain (Figure 4C). This cytosol remained active and hence stimulation cannot simply be due to the resupplying of Vrp1p. We also directly tested the effect of a semi-purified Vrp1p fraction, which consistently produced a slight enhancement of fusion (Figure 4, B and C). Therefore, Vrp1p might be one component of a complex mixture, though further studies will be needed to identify the other components. Las17p is a binding partner of Vrp1p and together are the yeast counterpart of the mammalian WASP/WIP complex, an essential component of the actin remodeling machinery (Higgs and Pollard, 2000). Interestingly, fusion of sterol-enriched vacuoles showed reduced sensitivity to Las17p antibodies, yet remained sensitive to SNARE antibodies and actin ligands (Figures 4A and 6), which is in accord with our suppressor studies. Therefore, the mechanism that is activated on sterol-enriched membranes, via *ERG6* overexpression, bypasses the actin regulatory mechanism at Vrp1p/Las17p, but promotes vacuole fusion through the normal pathway, which is both SNARE and actin dependent (Wickner, 2002).

This bypass result is much like the effect observed by overproduction of protein kinase activity, which suppressed endocytosis defects when sphingolipid synthesis was compromised (Friant *et al.*, 2000; 2001; Zanolari *et al.*, 2000). The sphingolipid requirement was linked to the need for proper actin organization by modulation of a signal transduction mechanism. Overexpression of the downstream kinases, Pkh1 or Pkh2, bypassed the need for sphingolipids (Friant *et al.*, 2001). These kinases activate Pkc1p, which is needed for correct cytoskeletal organization (Friant *et al.*, 2000). Conversely, our effect is to bypass the need for signaling proteins via membrane sterol enrichment. Though this is not the same lipid as in the former study, the functionality of sphingolipids and sterols are closely linked (Anderson and Jacobson, 2002). We speculate that a membrane-signaling platform is formed by organization of lipid subdomains. These platforms recruit and group signal transduction complexes to most efficiently produce downstream "work," this being signaling to membrane fusion in our case and to endocytosis in the former studies. Overproduction of the platform and work is recovered even if the signaling proteins are disrupted because more of the downstream components can be recruited. Conversely disruption the platform while overproducing the signaling complex also recovers the work.

Ergosterol Requirement for Vacuole Biogenesis

ERG6 overexpression led to changes in vacuole lipid composition resulting in an overall rise in vacuolar sterols (Table 4). The ergosterol biosynthetic pathway requires 21 enzymes to produce ergosterol from the initial condensation of acetyl-CoA (Daum *et al.*, 1998). HMG-CoA reductase (*HMG1*) is deemed to catalyze the rate-limiting step though overexpression of this enzyme, leading to increased levels of squalene, an upstream intermediate of ergosterol (Polakowski *et al.*, 1998). Systematic manipulation of post-squalene genes does not predict that *ERG6* overexpression would have a significant impact on total sterol levels (Veen *et al.*, 2003). Erg6p, which catalyzes the C24 methylation of zymosterol side-chain to produce fecosterol, is thought to be regulated by feedback inhibition by ergosterol (Venkatramesh *et al.*, 1996). Overproduction might alleviate this inhibition, resulting in increased ergosterol levels, a result reinforced by increased sensitivity to nystatin (Figure 9). *ERG6* overexpression was previously shown to produce only a small rise in cellular ergosterol levels, which differs from our findings (see Veen *et al.*, 2003 and Table 4). However, major strain differences must be taken into consideration. We used a genomic insertion of *GAL1* that could increase expression greater than 10-fold (Figure 3A), whereas Veen *et al.* (2003), using a high-copy plasmid, performed their analysis in an *HMG1* overproduction strain and did not examine levels of protein expression. We attained ~1.5-fold enrichment in vacuole sterols levels, which is a significant increase because ergosterol is not a major component of the vacuole membrane nor other intracellular organelles (Zinser *et al.*, 1991, 1993; Schneiter *et al.*, 1999). Ergosterol is needed for proper vacuole and mitochondrial biogenesis (Kato and Wickner, 2001; Dimmer *et al.*, 2002) and is required for protein sorting at the ER and Golgi mem-

brane (Bagnat *et al.*, 2000; Umebayashi and Nakano, 2003). Proper transcriptional regulation of *ERG* genes has also been shown to be necessary for vacuole assembly (Hongay *et al.*, 2002). Therefore, ergosterol is a vital component of membranes, even in organelles where it is not abundant. We believe it is the enrichment of ergosterol levels that stimulates fusion, which is supported by experiments showing differential strain sensitivity to nystatin (Figure 9). However, we cannot rule out that accumulation of other sterol intermediates such as fecosterol or a reduction of zymosterol might be the driving force behind our observations. Indeed, specific sterols are necessary at multiple steps of endocytosis (Munn *et al.*, 1999; Heese-Peck *et al.*, 2002). These studies showed the rate of receptor-mediated internalization could be correlated to structural differences of ergosterol intermediates with mutants in B-ring desaturases most strongly delayed.

Mechanism of Sterol-activated Fusion

We wanted to try and understand the mechanism of activated membrane fusion that is triggered by *ERG6* overexpression and membrane sterol enrichment. An ergosterol requirement for vacuole biogenesis had been previously shown (Munn *et al.*, 1999; Kato and Wickner, 2001; Hongay *et al.*, 2002). Several *erg* mutants have fragmented vacuoles and when purified are defective for homotypic fusion (Kato and Wickner, 2001). Our experiments also showed partial recovery of fusion after long preincubation periods with exogenously added cholesterol (Figure 2). To further explore the role of sterols, we pursued endogenous manipulation of sterols via *GAL1* induction experiments.

We first examined the effect of *ERG6* overexpression on vesicular trafficking. Characterization of the *vrp1*Δ strain identified a mild vacuolar-sorting defect. We thought that increased ergosterol levels (via *ERG6* overexpression) might lead to more efficient sorting and a correction of the *vrp1*Δ sorting defect—this in turn leading to stimulation of fusion. However direct comparison of strains with *ERG6* induced and uninduced showed little change in vacuolar protein sorting. Vacuole protein localization was recovered in some cases (Figure 8B, *Vam3p* and *Vph1p*); however, this was independent of *ERG6* induction, and CpY remained missorted to the plasma membrane (Figure 8A, compare YPD with YPG for *vrp1*Δ strains). We concluded that effects on protein sorting could not account for the large stimulation of membrane fusion.

We next examined the effect of vacuolar sterol enrichment on the kinetics of priming and bilayer fusion. During priming Sec17p is released from the *cis*-SNARE complex in a process catalyzed by Sec18p ATP hydrolysis. We showed that priming along with bilayer fusion is kinetically driven by *ERG6* overexpression (Figure 10, A and B). Vacuoles from the *vrp1*Δ strain did not efficiently release Sec17p during priming reactions; however, this was restored by *ERG6* overexpression (Figure 10C). Sterols have previously been shown to affect the function of membrane-bound ATPases (Cobon and Haslam, 1973). This may be related to the more efficient Sec18p ATPase-driven release of Sec17p from the vacuole membrane.

Actin and actin-remodeling proteins such as Vrp1p are localized to the vacuole membrane, and jasplakinolide, which stabilizes F-actin, inhibits the docking subreactions of membrane fusion (Eitzen *et al.*, 2002). This suggests that actin depolymerization is an early subreaction of membrane fusion in accord with an actin barrier model, which suggests actin must first be shed to allow membranes to be closely apposed. Here we show that actin is slowly released from vacuole membranes, and this reaction is slowed by deletion of *VRP1* (Figure 11). The activity was recovered by sterol enrichment to a level beyond that observe for wild-type vacuoles, in accord with increased fusion kinetics (Figure 10A). This is a good indication that control of actin organization is tightly coupled to the lipid environment of the membrane. However, we do not make any conclusion with this assay on the reformation of an actin network, and in fact this assay does not distinguish between changes in filamentous or globular actin (which are likely occurring). The simplest interpretation is that as actin is remodeled, transitions between globular and filamentous actin will cause some shedding to occur. Increased rate of remodeling would increase shedding, as detected in our assay.

ACKNOWLEDGMENTS

We thank Drs. Günter Daum, David Drubin, Rachard Rachubinski, Howard Riezman, William Wickner, and Rick Wozniak for yeast strains and reagents. We thank Dr. Andrew Simmonds for critical readings of this manuscript. This work was supported by grants to G.E. from the Canadian Institutes of Health Research (CIHR) and the Alberta Heritage Foundation for Medical Research and a grant to R.L. from the Heart and Stroke Foundation of Alberta. R.L. and G.E. are AHFMR Scholars and G.E is a CIHR New Investigator.

REFERENCES

Anderson, R.G., and Jacobson, K. (2002). A role for lipid shells in targeting proteins to caveolae, rafts, and other lipid domains. Science *296*, 1821–1825.

Anes, E., Kuhnel, M.P., Bos, E., Moniz-Pereira, J., Habermann, A., and Griffiths, G. (2003). Selected lipids activate phagosome actin assembly and maturation resulting in killing of pathogenic mycobacteria. Nat. Cell Biol. *5*, 793–802.

Ausubel, F.J., Brent, R., Kingston, R.E., Moore, D.D., Seidman, J.G., Smith, J.A., and Struhl, K. (1989). Current Protocols in Molecular Biology, New York: Green Publishing Associates, Section 13.7.

Bagnat, M., Keranen, S., Shevchenko, A., Shevchenko, A., and Simons, K. (2000). Lipid rafts function in biosynthetic delivery of proteins to the cell surface in yeast. Proc. Natl. Acad. Sci. USA *97*, 3254–3259.

Bernstein, B.W., DeWit, M., and Bamburg, J.R. (1998). Actin disassembles reversibly during electrically induced recycling of synaptic vesicles in cultured neurons. Brain Res. Mol. Brain Res. *53*, 236–251.

Brachmann, C.B., Davies, A., Cost, G.J., Caputo, E., Li, J., Hieter, P., and Boeke, J.D. (1998). Designer deletion strains derived from *Saccharomyces cerevisiae* S288C: a useful set of strains and plasmids for PCR-mediated gene disruption and other applications. Yeast *14*, 115–132.

Cobon, G.S., and Haslam, J.M. (1973). The effect of altered membrane sterol composition on the temperature dependence of yeast mitochondrial ATPase. Biochem. Biophys. Res. Commun. *52*, 320–326.

Daum, G., Lees, N.D., Bard, M., and Dickson, R. (1998). Biochemistry, cell biology and molecular biology of lipids of *Saccharomyces cerevisiae*. Yeast *14*, 1471–1510.

Defacque, H. *et al.* (2000). Involvement of ezrin/moesin in de novo actin assembly on phagosomal membranes. EMBO J. *19*, 199–212.

Dimmer, K.S., Fritz, S., Fuchs, F., Messerschmitt, M., Weinbach, N., Neupert, W., and Westermann, B. (2002). Genetic basis of mitochondrial function and morphology in *Saccharomyces cerevisiae*. Mol. Biol. Cell *13*, 847–853.

Duncan, M.C., Cope, M.J., Goode, B.L., Wendland, B., and Drubin, D.G. (2001). Yeast Eps15-like endocytic protein, Pan1p, activates the Arp2/3 complex. Nat. Cell Biol. *3*, 687–690.

Eitzen, G. (2003). Actin remodeling to facilitate membrane fusion. Biochim. Biophys. Acta *1641*, 175–181.

Eitzen, G., Wang, L., Thorngren, N., and Wickner, W. (2002). Remodeling of organelle-bound actin is required for yeast vacuole fusion. J. Cell Biol. *158*, 669–679.

Eitzen, G., Thorngren, N., and Wickner, W. (2001). Rho1p and Cdc42p act after Ypt7p to regulate vacuole docking. EMBO J. *20*, 5650–5656.

Evangelista, M., Klebl, B.M., Tong, A.H., Webb, B.A., Leeuw, T., Leberer, E., Whiteway, M., Thomas, D.Y., and Boone, C. (2000). A role for myosin-I in actin assembly through interactions with Vrp1p, Bee1p, and the Arp2/3 complex. J. Cell Biol. *148*, 353–362.

Friant, S., Lombardi, R., Schmelzle, T., Hall, M.N., and Riezman, H. (2001). Sphingoid base signaling via Pkh kinases is required for endocytosis in yeast. EMBO J. *20*, 6783–6792.

Friant, S., Zanolari, B., and Riezman, H. (2000). Increased protein kinase or decreased PP2A activity bypasses sphingoid base requirement in endocytosis. EMBO J. *19*, 2834–2844.

Gavin, A.C. *et al.* (2002). Functional organization of the yeast proteome by systematic analysis of protein complexes. Nature *415*, 141–147.

Haas, A. (1995). A quantitative assay to measure homotypic fusion in vitro. Methods Cell Sci. *17*, 283–294.

Heese-Peck, A., Pichler, H., Zanolari, B., Watanabe, R., Daum, G., and Riezman, H. (2002). Multiple functions of sterols in yeast endocytosis. Mol. Biol. Cell *13*, 2664–2680.

Higgs, H.N., and Pollard, T.D. (2000). Activation by Cdc42 and PIP2 of Wiskott-Aldrich syndrome protein (WASp) stimulates actin nucleation by Arp 2/3 complex. J. Cell Biol. *150*, 1311–1320.

Hongay, C., Jia, N., Bard, M., and Winston, F. (2002). Mot3 is a transcriptional repressor of ergosterol biosynthetic genes and is required for normal vacuolar function in *Saccharomyces cerevisiae.* EMBO J. *21*, 4114–4124.

Ikonen, E. (2001). Role of lipid rafts in membrane fusion. Curr. Opin. Cell Biol. *13*, 470–477.

Jahn, R., and Sudhof, T.C. (1999). Membrane fusion and exocytosis. Annu. Rev. Biochem. *68*, 863–911.

Jahn, R., Lang, T., and Sudhof, T.C. (2003). Membrane fusion. Cell *112*, 519–533.

Jahraus, A. *et al.* (2001). ATP-dependent membrane assembly of F-actin facilitates membrane fusion. Mol. Biol. Cell *12*, 155–170.

Kato, M., and Wickner, W. (2001). Ergosterol is required for the Sec18/ATP-dependent priming step of homotypic vacuole fusion. EMBO J. *20*, 4035–4040.

Kjeken, R. *et al.* (2004). Fusion between phagosomes, early and late endosomes: a role for actin in fusion between late, but not early endocytic organelles. Mol. Biol. Cell *15*, 345–358.

Koning, A.J., Larson, L.L., Cadera, E.J., Parrish, M.L., and Wright, R.L. (2002). Mutations that affect vacuole biogenesis inhibit proliferation of the endoplasmic reticulum in *Saccharomyces cerevisiae.* Genetics *160*, 1335–1352.

Kucharczyk, R., Dupre, S., Avaro, S., Haguenauer-Tsapis, R., Slonimski, P.P., and Rytka, J. (2000). The novel protein Ccz1p required for vacuolar assembly in *Saccharomyces cerevisiae* functions in the same transport pathway as Ypt7p. J. Cell Sci. *113*, 4301–4311.

Longtine, M.S., McKenzie, A., 3rd, Demarini, D.J., Shah, N.G., Wach, A., Brachat, A., Philippsen, P., and Pringle, J.R. (1998). Additional modules for versatile and economical PCR-based gene deletion and modification in *Saccharomyces cerevisiae.* Yeast *14*, 953–961.

Mayer, A. (2002). Membrane fusion in eukaryotic cells. Annu. Rev. Cell Dev. Biol. *18*, 288–314.

Mayer, A., Wickner, W., and Haas, A. (1996). Sec18p (NSF)-driven release of Sec17p (alpha-SNAP) can precede docking and fusion of yeast vacuoles. Cell *85*, 83–94.

Muallem, S., Kwiatkowska, K., Xu, X., and Yin, H.L. (1995). Actin filament disassembly is a sufficient final trigger for exocytosis in nonexcitable cells. J. Cell Biol. *128*, 589–598.

Müller, O., Johnson, D.I., and Mayer, A. (2001). Cdc42p functions at the docking stage of yeast vacuole membrane fusion. EMBO J. *20*, 5657–5665.

Munn, A.L., Heese-Peck, A., Stevenson, B.J., Pichler, H., and Riezman, H. (1999). Specific sterols required for the internalization step of endocytosis in yeast Mol. Biol. Cell *10*, 3943–3957.

Myher, J.J., Kuksis, A., and Pind, S. (1989). Molecular species of glycerophospholipids and sphingomyelins of human plasma: comparison to red blood cells. Lipids *24*, 408–418.

Parks, L.W., Crowley, J.H., Leak, F.W., Smith, S.J., and Tomeo, M.E. (1999). Use of sterol mutants as probes for sterol functions in the yeast, *Saccharomyces cerevisiae.* Crit. Rev. Biochem. Mol. Biol. *34*, 399–404.

Polakowski, T., Stahl, U., and Lang, C. (1998). Overexpression of a cytosolic hydroxymethylglutaryl-CoA reductase leads to squalene accumulation in yeast. Appl. Microbiol. Biotechnol. *49*, 66–71.

Roberts, C.J., Raymond, C.K., Yamashiro, C.T., and Stevens, T.H. (1991). Methods for studying the yeast vacuole. Methods Enzymol. *194*, 644–661.

Schaerer-Brodbeck, C., and Riezman, H. (2000). Saccharomyces cerevisiae Arc35p works through two genetically separable calmodulin functions to regulate the actin and tubulin cytoskeletons. J. Cell Sci. *113*, 521–532.

Schneiter, R. *et al.* (1999). Electrospray ionization tandem mass spectrometry (ESI-MS/MS) analysis of the lipid molecular species composition of yeast subcellular membranes reveals acyl chain-based sorting/remodeling of distinct molecular species en route to the plasma membrane. J. Cell Biol. *146*, 741–754.

Seeley, E.S., Kato, M., Margolis, N., Wickner, W., and Eitzen, G. (2002). Genomic analysis of homotypic vacuole fusion. Mol. Biol. Cell *13*, 782–794.

Segev, N. (2001). Ypt/rab GTPases: regulators of protein trafficking. Sci. STKE *2001*, RE11.

Stamnes, M. (2002). Regulating the actin cytoskeleton during vesicular transport. Curr. Opin. Cell Biol. *14*, 428–433.

Symons, M., and Rusk, N. (2003). Control of vesicular trafficking by Rho GTPases. Curr. Biol. *13*, R409–R418.

Umebayashi, K., and Nakano, A. (2003). Ergosterol is required for targeting of tryptophan permease to the yeast plasma membrane. J. Cell Biol. *161*, 1117–1131.

Veen, M., Stahl, U., and Lang, C. (2003). Combined overexpression of genes of the ergosterol biosynthetic pathway leads to accumulation of sterols in *Saccharomyces cerevisiae.* FEMS Yeast Res. *4*, 87–95.

Venkatramesh, M., Guo, D.A., Harman, J.G., and Nes, W.D. (1996). Sterol specificity of the *Saccharomyces cerevisiae ERG6* gene product expressed in *Escherichia coli.* Lipids *31*, 373–377.

Vitale, M.L., Rodriguez Del Castillo, A., Tchakarov, L., and Trifaro, J.M. (1991). Cortical filamentous actin disassembly and scinderin redistribution during chromaffin cell stimulation precede exocytosis, a phenomenon not exhibited by gelsolin. J. Cell Biol. *113*, 1057–1067.

Wang, L., Merz, A.J., Collins, K.M., and Wickner, W. (2003). Hierarchy of protein assembly at the vertex ring domain for yeast vacuole docking and fusion. J. Cell Biol. *160*, 365–374.

Wang, L., Seeley, E.S., Wickner, W., and Merz, A.J. (2002). Vacuole fusion at a ring of vertex docking sites leaves membrane fragments within the organelle. Cell *108*, 357–369.

Weisman, L.S., Bacallao, R., and Wickner, W. (1987). Multiple methods of visualizing the yeast vacuole permit evaluation of its morphology and inheritance during the cell cycle. J. Cell Biol. *105*, 1539–1547.

Wickner, W. (2002). Yeast vacuoles and membrane fusion pathways. EMBO J. *21*, 1241–1247.

Zanolari, B., Friant, S., Funato, K., Sutterlin, C., Stevenson, B.J., and Riezman, H. (2000). Sphingoid base synthesis requirement for endocytosis in Saccharomyces cerevisiae. EMBO J. *19*, 2824–2833.

Zinser, E., Paltauf, F., and Daum, G. (1993). Sterol composition of yeast organelle membranes and subcellular distribution of enzymes involved in sterol metabolism. J. Bacteriol. *175*, 2853–2858.

Zinser, E., Sperka-Gottlieb, C.D., Fasch, E.V., Kohlwein, S.D., Paltauf, F., and Daum, G. (1991). Phospholipid synthesis and lipid composition of subcellular membranes in the unicellular eukaryote *Saccharomyces cerevisiae.* J. Bacteriol. *173*, 2026–2034.